THE ASTROPHYSICAL JOURNAL, 461:750–761, 1996 April 20

THE DISCOVERY OF HOT STARS NEAR THE GALACTIC CENTER THERMAL RADIO FILAMENTS

ANGELA S. COTERA,[1] EDWIN F. ERICKSON,[2] SEAN W. J. COLGAN,[2,3] JANET P. SIMPSON,[2,4]
DAVID A. ALLEN,[5,6] AND MICHAEL G. BURTON[7]
Received 1994 December 21; accepted 1995 September 25

ABSTRACT

We report the discovery of a highly unusual cluster of stars at G0.121+0.017 near the Arched (thermal) Filaments, ~10′ northeast of the Galactic center. *H* (1.65 μm) and *K′* (2.1 μm) images are used to estimate a distance to the cluster consistent with a Galactic center location. *K′*-band spectroscopy reveals that the cluster contains 13 stars with Brγ (2.166 μm) emission: 12 of these stars also have He I (2.112/3 μm) emission, and two show fainter He II (2.189 μm) emission. Based on a spectral comparison with optically classified stars, we suggest the new emission stars are late WN stars. If the classification is correct, the cluster contains ~14% of all known Galactic WN stars.

Observations of emission-line stars near G0.15−0.05, the "Pistol," are also presented. There are four stars near the Pistol which contain emission lines. Three of these stars differ spectroscopically from the stars in the new cluster; one has a spectrum that is similar to the new cluster stars. Together with the cluster stars, these newly discovered hot young stars provide evidence for recent star formation and the stellar ionization of the thermal radio emission regions in the vicinity of the Galactic center.

Subject headings: Galaxy: center — infrared: stars — open clusters and associations: individual (G0.121+0.017) — stars: Wolf-Rayet

1. INTRODUCTION

Since the Galactic center (GC) is undetectable at visible wavelengths as a result of interstellar extinction, investigations of the nearest galactic nucleus must rely extensively on radio and infrared observations. Radio continuum maps first revealed the unusual morphology of the regions known as the Straight (nonthermal emission) and Arched (thermal emission) Filaments at a projected distance ~30 pc from the GC (Yusef-Zadeh, Morris, & Chance 1984; Morris & Yusef-Zadeh 1985). The presence of magnetic fields, strongly suggested by the morphology, is supported by far-infrared (FIR) polarization observations along the filaments (Morris et al. 1992). Estimates suggest a magnetic strength of at least 1 mG (Yusef-Zadeh & Morris 1987a, b).

The primary excitation mechanism of the GC arched filaments is uncertain. It has been argued that the ionization is the result of an interaction between the magnetic field and a molecular cloud coincident with the filaments (Serabyn & Güsten 1987; Morris & Yusef-Zadeh 1989). Alternatively, it has been suggested that photoionization by hot stars is responsible for the observed radio emission (e.g., Erickson et al. 1991). Morris & Yusef-Zadeh (1989) argued that photoionization by OB stars is unlikely on morphological grounds, but their magnetohydrodynamic induced ionization models fail to produce the observed infrared continuum luminosity (Erickson et al. 1991).

In the past few years, advances in infrared array technology have greatly increased the spatial and spectral resolution in the near-infrared (NIR), providing a powerful tool to study the GC. Recent NIR observations of the central few parsecs of the Galaxy revealed a compact ($r \sim 1$ pc) cluster of approximately a dozen hot stars, $\sim 10^7$ yr old (Allen 1994; Krabbe et al. 1991; Allen, Hyland, & Hillier 1990), supporting the hypothesis that there has been a recent episode of star formation in that region. However, the central few parsecs are largely devoid of molecular gas such that conventional star formation seems unlikely. It has been suggested that the luminous stars there are the result of the unique and tumultuous conditions in the area immediately surrounding Sgr A* and unrelated to general star formation in the vicinity of the GC (Morris 1993). The infall time for stars $\gtrsim 3$ pc from the GC prohibits migration or segregation toward the center as a possible explanation of the origin of the stars, prompting Genzel, Hollenbach, & Townes (1994) to speculate that stellar mergers could be responsible for the production of the massive stars within the central parsec. The discovery of similarly hot massive stars near the Arched Filaments presented here suggests that these explanations are insufficient.

Within the central 100 pc, but outside the central cavity, the requisite large-scale structures associated with stellar formation are certainly present: large molecular clouds (Serabyn & Güsten 1987, 1991) and extended regions of thermal radio emission (Yusef-Zadeh & Morris 1987a, b) whose far-infrared spectrum is typical of H II regions (Erickson et al. 1991). However, other indicators of star formation, such as OH masers, are absent (Morris 1989). In addition, the unusual filamentary morphology of the ionized gas, atypical of galactic H II regions, argues against star formation (Morris & Yusef-Zadeh 1989). To illustrate the difficulty of forming stars in the region, consider that extreme tidal forces imply a Jeans mass of $\sim 10^5$–10^7 $M_{\odot}$ and increase the lower limit for the initial stellar mass to ~ 1 $M_{\odot}$ (Morris 1993). The complexity of the region precludes simple explanations, and the hypothesis of recent or ongoing star formation has not been universally accepted.

[1] Stanford University, Applied Physics Department, Stanford, CA 94305.
[2] NASA/Ames Research Center, MS 245-6, Moffett Field, CA 94035.
[3] The SETI Institute.
[4] University of California, Berkeley.
[5] Deceased 1994 July 26, depriving us prematurely of a versatile and capable astronomer and a good friend to many of us.—Editor.
[6] Anglo-Australian Observatory.
[7] University of New South Wales, School of Physics, P.O. Box 1, 2033 Kensington, NSW, Australia.

Previous photometric observations of portions of the Arched Filaments had proved insufficient to classify the stars in the region owing to the uncertainties introduced by crowding and variable extinction (Cotera et al. 1992). Therefore, NIR spectral data were obtained in the H and K bands, which contain several stellar emission and absorption lines useful in distinguishing hot stars from cool stars (Hillier 1985; Allen et al. 1990; Hanson & Conti 1994). In their study of the stellar cluster in the central parsec, Burton and Allen (1992) used the He I (2.058 μm) emission line to identify the hot young stars. We have applied this method, using both the He I (2.058 μm) and Brγ (2.166 μm) lines, to investigate the existence of hot stars in the vicinity of the Arched Filaments.

To date, our observations have revealed $\sim$22 hot stars within the inner $\sim$40 pc of the Galaxy and have provided additional information on the emission-line stars in and near the previously studied GC cluster of stars known as AFGL 2004 (Glass, Moneti, & Moorwood 1990; Nagata et al. 1990; Okuda et al. 1990; Moneti, Glass, & Moorwood 1994; Harris et al. 1994). Here we discuss a new cluster of emission-line stars located at G0.121+0.017, hereafter referred to as the G0.12+0.02 cluster, the emission-line stars near the radio emission region G0.15−0.05, the "Pistol" (nomenclature from Yusef-Zadeh & Morris 1987a), and a few optically classified O and WN stars whose spectra were obtained during these observations to aid in the classification of the newly discovered stars. The observations and data reduction techniques are described in § 2; the results of the observations are presented in § 3; an estimate of the luminosity and associated UV flux is given in § 4; and our conclusions are presented in § 5.

2. OBSERVATIONS AND DATA REDUCTION

Observations were made at the Anglo-Australian Observatory on 1992 July 13–14 and 1993 June 13–15 with the facility Infrared Imaging Spectrometer IRIS which utilizes a Rockwell 128 × 128 pixel HgCdTe (NICMOS II) array. The 0".6 pixel^{-1} scale was selected for all observations. The K' band (central wavelength 2.1 μm; Wainscoat & Cowie 1992) was used rather than the K (2.2 μm) band because it significantly lowers the thermal component of the background (differences in the photometric measurements of K and K' are discussed in § 3.1). All data were linearized, bias subtracted, flat-fielded, and sky-subtracted with the astronomical software reduction package FIGARO.

The combined broadband J, H, and K' image of the region near the G0.12+0.02 cluster is presented in Figure 1 (Plate 15) overlain on the 20 cm radio map contours (Morris & Yusef-Zadeh 1989). The figure is a mosaic of 32 images, 70" × 70" each, in J, H, and K' which are combined in a three-color composite. Additional J, H, and K' images were taken with the G0.12+0.02 cluster at several locations on the array to reduce errors due to variations in pixel responsivity. These broadband images of the cluster were obtained during excellent seeing, resulting in a measured FWHM of $\sim$0".9. Photometry results for the cluster were obtained using these images and IRAF/DAOPHOT. There are $\sim$400 stars in each 70" × 70" image at K', which makes precise magnitudes difficult to obtain because of crowding. Our sensitivity for these observations was $m_{K'} \gtrsim 9.5$ because of saturation and $m_{K'} \lesssim 16.0$ because of crowding.

Spectroscopic observations of the G0.12+0.02 cluster and the Pistol utilized data cubes, with axes α, δ, and λ. The data cubes were obtained by observing in spectral mode with a 70" × 2".0 slit (resolution $R \sim 250$) at fixed right ascension, while the telescope drifted in declination at a rate of 36" hr^{-1}. Spectral images of each source were extracted from the data cubes by co-adding the desired α, δ planes (usually three planes centered on the emission wavelength) and using adjacent planes, containing no emission-line features, for sky continuum subtraction. The Brγ emission image of the G0.12+0.02 cluster is shown in Figure 2*a* (Plate 16) with a schematic of the cluster given in Figure 2*b*. The Brγ image of the region surrounding the Pistol is shown in Figure 3 (Plate 17). The emission-line images were used to locate hot stars, which appear as strong compact sources in the images.

The spectrum of an individual star can also be extracted from the data cube by locating the star along the δ axis of the cube and co-adding the α, λ planes containing the star. After the α, λ plane has been extracted from the cube, the rows in the plane which contain the star are extracted, and the sky continuum is subtracted by using adjacent rows in the plane that are free of stars. The spectral resolution for this method is $\sim$250. Spectra of several G0.12+0.02 cluster stars and Pistol emission-line stars were obtained in this way.

Higher resolution spectra of some individual stars were taken by first placing the star at one end of a 21" × 0".5 slit, $R \gtrsim 350$, then at the other end and subtracting one observation from the other. This results in a single image with the star appearing as both a positive and negative feature. After the image has been flat-fielded, the positive and negative spectra of the star were extracted and differenced, improving the signal-to-noise ratio and removing night-sky lines and sky continuum. The spectra of most of the G0.12+0.02 cluster stars, the bright compact source below the Pistol, and optically classified stars were obtained by this method.

Spectra of main-sequence early G standards located near the program sources were used for all flux calibrations (Allen & Craig 1983). The flux calibration routine assumes that the star radiates as a blackbody, and we used a temperature of 5600 K for all G standards (Allen 1976b).

3. RESULTS

3.1. *Photometry*

The photometric image of the regions surrounding the Arched Filaments (Fig. 1) shows the G0.12+0.02 cluster, located at R.A. (1950) $17^{h}42^{m}40^{s}.0$, decl. $-28°48'19"$. Table 1 gives the measured magnitudes of the stars within a 30" radius of the center of the cluster. The average estimated error for these magnitudes is ± 0.25, which is largely due to crowding in the region. In Table 1 and in Figure 2*b*, the numbered stars indicate those with emission-line features, while letters indicate those without significant emission lines whose position suggest a possible association with the cluster.

The results of the photometry are presented in Figure 4, where we have plotted K magnitudes versus $H-K$ colors for stars common to three of the G0.12+0.02 cluster images. To allow a comparison to published data, the measured K' magnitudes have been adjusted to K magnitudes for this figure using the equation from Wainscoat & Cowie (1992) which relates K and K', based on the central wavelengths of H (1.65 μm), K (2.22 μm), and K' (2.11 μm) bands:

$$K = \frac{1}{0.81}(K' - 0.19H) . \quad (1)$$

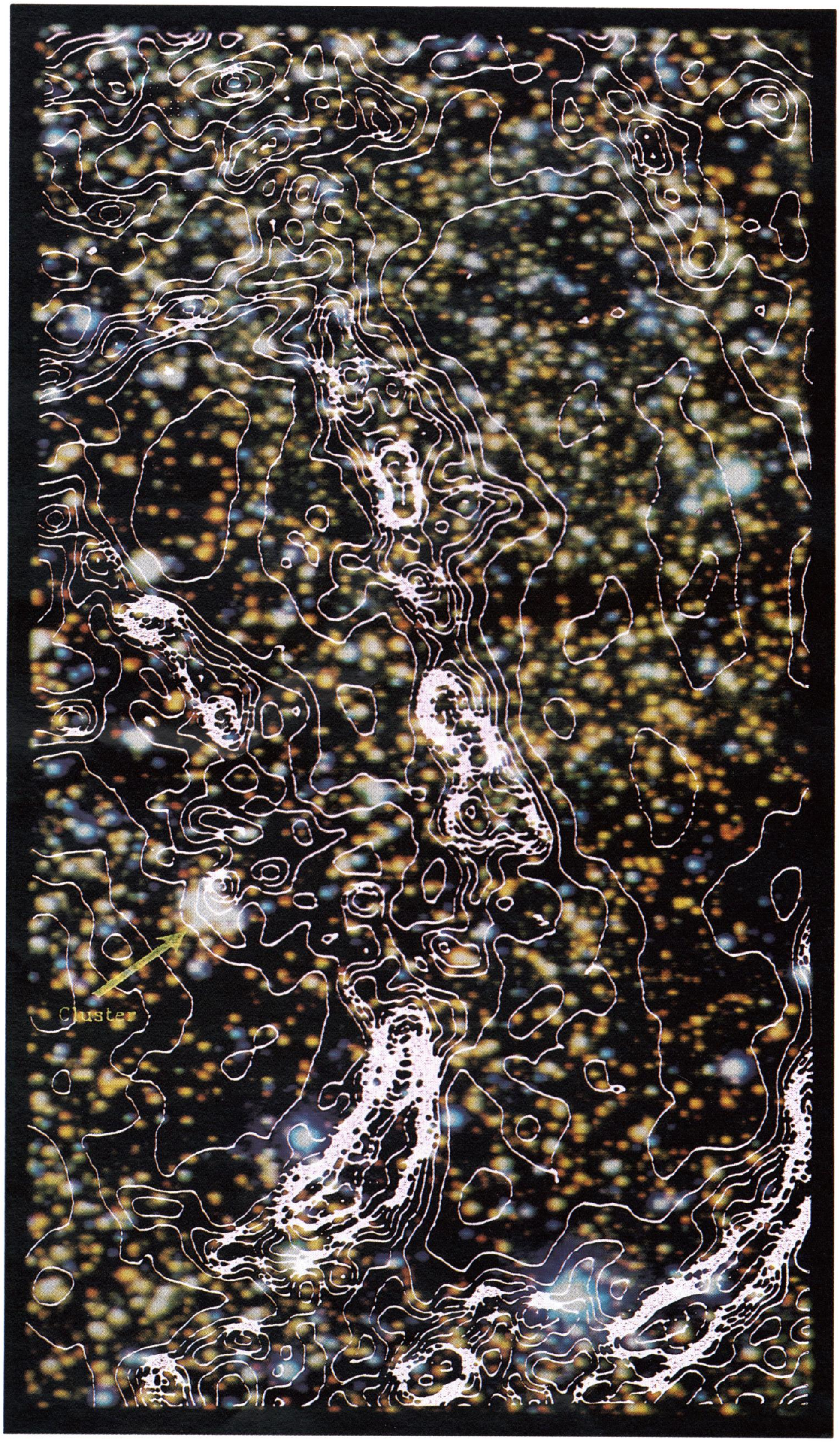

FIG. 1.—Three-color JHK' broadband composite of the region surrounding the arched filaments overlayed with the radio map (Morris & Yusef-Zadeh 1989). The G0.12 + 0.02 cluster stars discussed in this paper are seen on the lower left and labeled with a green arrow.

COTERA et al. (see 461, 751)

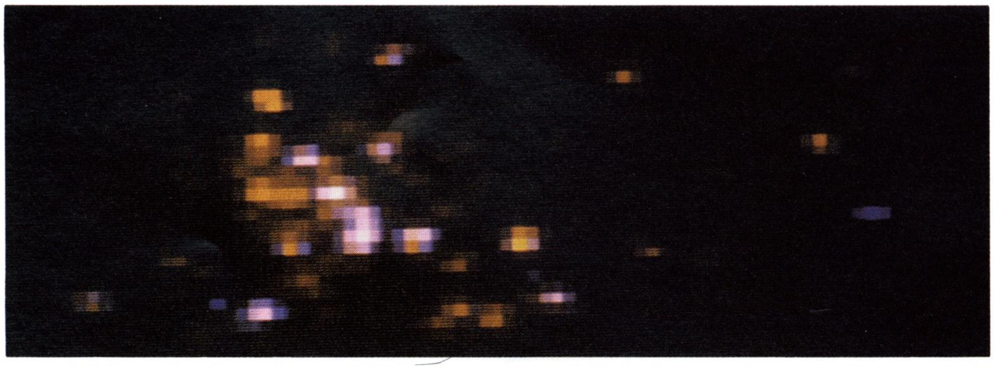

FIG. 2*a*

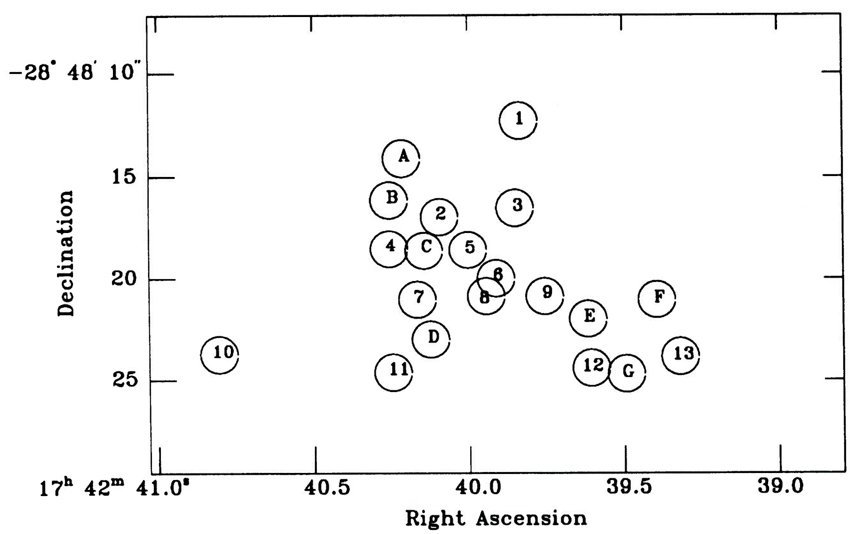

FIG 2*b*

FIG. 2.—(*a*) Two-color composite of the cluster of emission stars produced by combining the continuum image with the image of the Brγ emission. The white stars are those with Brγ emission whose spectra are given in Figs. 6–7; the yellow stars have no Brγ emission. (*b*) Schematic of cluster stars. Numbers indicate stars with emission lines, letters identify stars with featureless spectra.

COTERA et al. (see 461, 751)

1996ApJ...461..750C

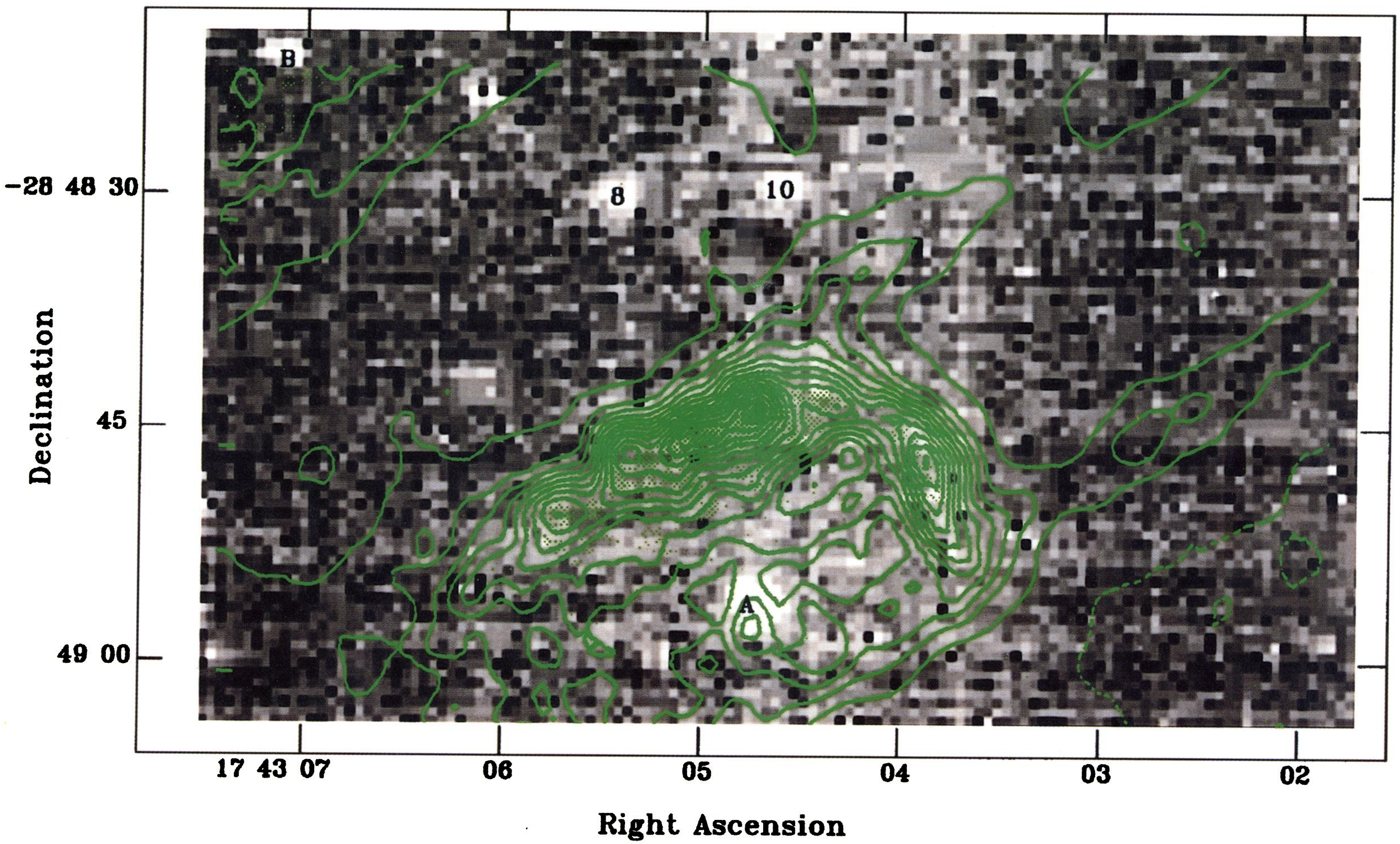

FIG. 3.—Brγ emission image from the Pistol and surrounding area. The image has been overlain with the radio continuum map (Yusef-Zadeh & Morris 1987a). The stars immediately above the Pistol are, from right to left, AFGL 2004 numbers 8 and 10 as identified by Glass et al. (1990). The star in the upper left corner is source B, a newly discovered star. The star beneath the Pistol is source A.

COTERA et al. (see 461, 751)

TABLE 1

PHOTOMETRY OF G0.12+0.02 CLUSTER STARS

Star	K'	$H-K'$	$J-K'$
1..............	10.6	1.5	4.5
2..............	10.2	1.5	4.6
3..............	10.6	1.4	4.5
4..............	11.0	1.1	4.1
5..............	9.7	1.6	4.7
7..............	10.7	1.5	4.6
8..............	10.1	1.4	4.7
9..............	10.2	1.7	5.0
10..............	11.3	1.8	5.3
11..............	10.3	1.5	4.9
12..............	11.0	1.7	5.2
13..............	10.7	2.0	5.8
A	10.2	1.9	6.0
B..............	10.6	1.4	4.4
C	10.7	1.4	4.3
D	11.4	1.5	4.6
E..............	11.5	1.7	5.1
F..............	10.3	0.3	1.3
G	10.8	1.4	5.6

To determine the location of the cluster along the line of sight, we estimate the extinction from the reddening curves of Catchpole, Whitelock, & Glass (1990) as shown in Figure 4. Catchpole et al. found that the extinction toward the GC was $A_V \sim 25$–35; from Figure 4, the G0.12+0.02 cluster falls within this range. As can be seen in Table 1 and Figure 4, at least one star within the 30″ cluster radius (star F) appears to be a foreground star.

For comparison, the stars from AFGL 2004 cluster are also plotted in Figure 4 using the data of Moneti et al. (1994). Glass et al. (1990) and Okuda et al. (1990) suggest that AFGL 2004 is located in the Galactic center based on the interstellar extinction derived from color determinations and on the 10 μm optical depth determined from observations of silicate features. Although $H-K$ values for many of the stars in AFGL 2004 are considerably larger than the G0.12+0.02 cluster stars, the stars in both clusters

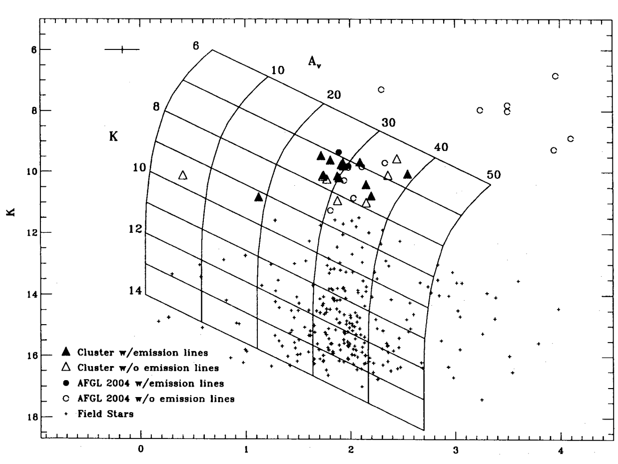

FIG. 4.—K vs. $H-K$ for the G0.12+0.02 cluster region and the AFGL 2004 cluster. The curves show the expected location of the giant branch, using 47 Tuc as a reference, for various values of the mean interstellar extinction based on the analysis of Galactic center stars of Catchpole et al. (1990). Triangles indicate the G0.12+0.02 cluster stars; circles indicate the value for the stars in the AFGL 2004 cluster. Filled triangles and circles are emission-line stars. Crosses indicate field stars not associated with the G0.12+0.02 cluster. Error bars are given in the upper left corner.

which exhibit K-band emission lines are located within the same magnitude and $H-K$ range. Thus, from an estimate of visual extinction and the agreement of these values with similar stars accepted as GC sources, the G0.12+0.02 cluster of emission stars is very likely located near the GC.

3.2. *Spectroscopy*

In the Brγ emission image of the cluster (Fig. 2*a*), strong emission is seen in highly compact objects, with confusion only in the most crowded regions. We believe that the emission is stellar in origin. If the Brγ emission were coming instead from an H II region, assuming case B recombination with $T_e = 10^4$ K and $N_e = 10^4$ cm^{-3}, and correcting for extinction in the Brγ line flux, we predict a 6 cm flux of ~ 10 mJy. Using our beam size to convert the predicted flux to the flux measured at 6 cm using the Very Large Array (VLA) with a 3″.8 × 3″.1 beam (Morris & Yusef-Zadeh 1989), we predict a flux of ~ 100 mJy beam^{-1}. No 6 cm emission is detected at the location of the cluster, although features of 50 mJy beam^{-1} are seen nearby.

Spectra of the G0.12+0.02 cluster stars are presented in Figure 5, and the line fluxes for the emission stars are presented in Table 2. In the K band, 12 of the 13 cluster stars with Brγ (2.166 μm) emission also have an emission line at 2.113 μm, with two possibly having the He II (2.189 μm) line in emission. In their recent work on the spectral classification of OB stars, Hanson & Conti (1994) detect an N III (2.116 μm) in emission in several of the stars. At our resolution, the measured line flux at 2.113 μm could be enhanced by the N III line; however, we are unable to discriminate between He I and N III because of line broadening, which is likely produced by stellar winds. As three of the stars have the He I 1.700 μm line in addition to the He II line, and the observed line is at exactly the same wavelength in the optically classified reference stars, we believe the line to be the He I 2.112/3 doublet line. In addition, it should be noted that there are two more emission lines coincident with the Brγ 2.166 μm line: He I (7–4) and He II (14–8). For the stars we have observed, the contribution by He II is likely negligible based on the weak He II (10–7) 2.189 μm line. However, the He I (7–4) contribution may be significant if the 2.113 μm feature is due entirely to He I as opposed to N III. In the H band, most of the emission-line stars show the Brackett lines, with the 1.736 μm H (10–4) line clearly visible in all of the spectra. The K-band spectra of cluster stars 6, A, and E (Figs. 5*b* and 5*d*) were extracted from the data cube of the cluster; therefore, no H-band data are presented, and the spectra are at a lower resolution than the other stars. Star A has deep CO (2.298 μm) band head absorption features in conjunction with possible Brγ emission, although at this resolution the Brγ feature is $\lesssim 2\ \sigma$.

After the 1992 discovery of the emission-line stars in the G0.12+0.02 cluster, the unusual nature of their K-band emission and the lack of stars with similar spectra in the literature prompted our observations of several optically classified (van der Hucht et al. 1981) stars to aid in classifying the cluster stars. Since the time of our initial observations, several groups have obtained H- and K-band spectra of O supergiant and WN stars (e.g., Conti et al. 1995; Crowther 1995) at higher resolution than the spectra presented here. The spectra of the optically classified stars observed during this work are shown in Figure 6, and the line fluxes are given in Table 3. In Figure 7, the spectra of a typical cluster star, and an optically classified WN 9 star,

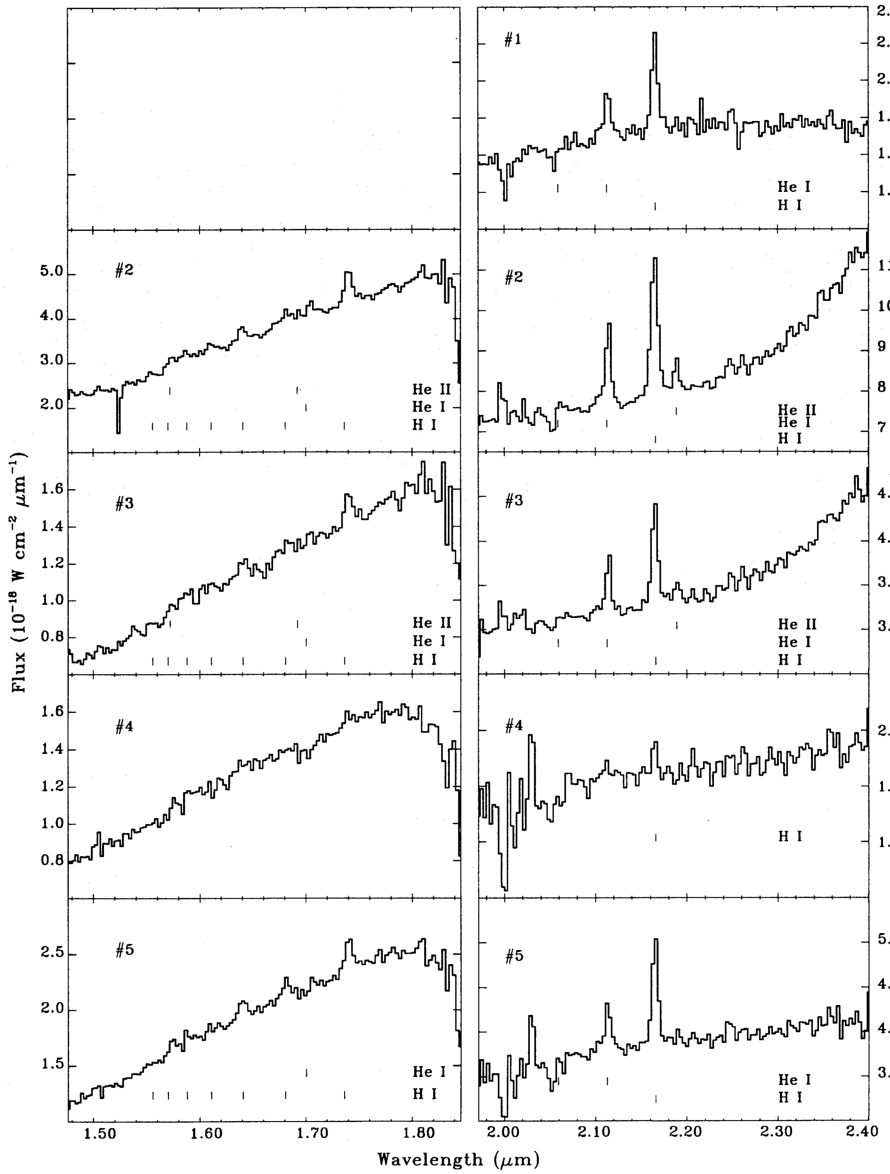

FIG. 5*a*

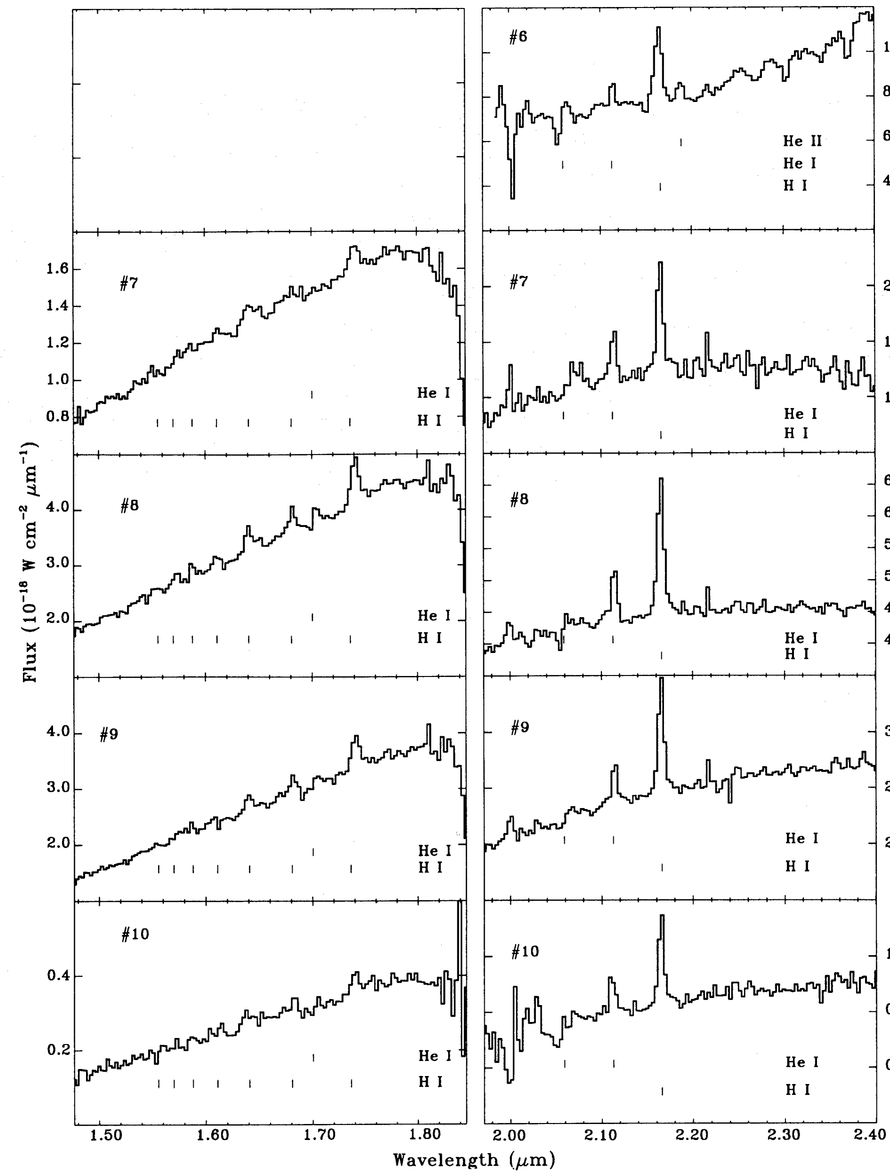

FIG. 5*b*

FIG. 5.—(*a*) *H*- and *K*-band spectra of the G0.12 + 0.02 cluster emission stars as labeled in Fig. 2*b*. Identifiable in all the stars are the hydrogen bracket lines, with Brγ (2.166 μm) the strongest of these lines, and the He I (2.112/3 μm) emission line. Two also have He II (2.189 μm) emission. The line positions are indicated by the vertical lines at the bottom of the spectra. Line fluxes are given in Table 2. (*b*) *H*- and *K*-band spectra of the G0.12 + 0.02 cluster emission stars. (*c*) *H*- and *K*-band spectra of the G0.12 + 0.02 cluster emission stars. (*d*) *K*-band spectra of two non-emission G0.12 + 0.02 cluster stars. The spectra were extracted from the data cube taken in 1992 July and are therefore at lower resolution (~250).

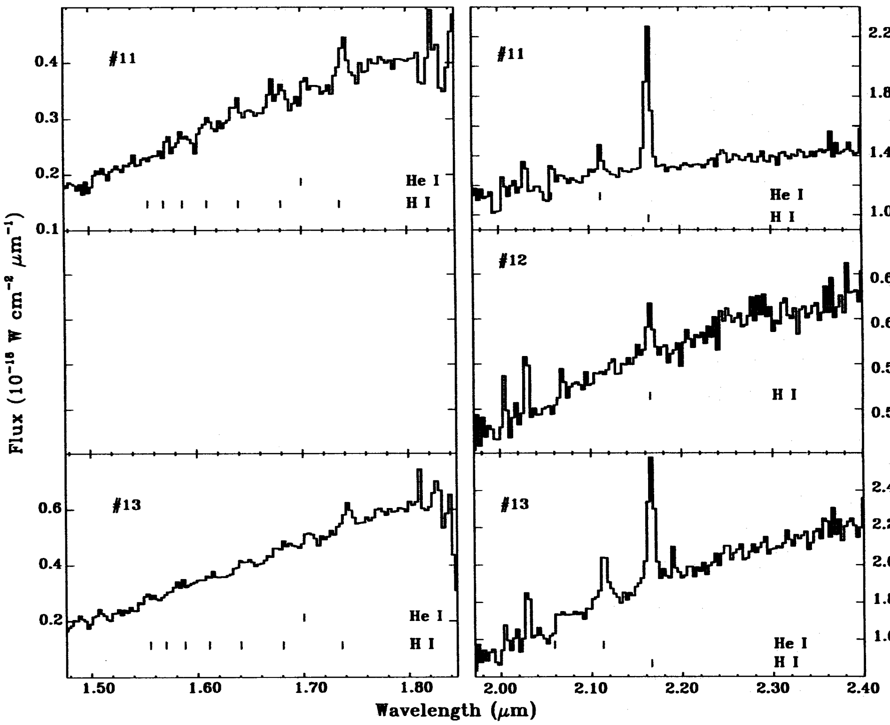

FIG. 5*c*

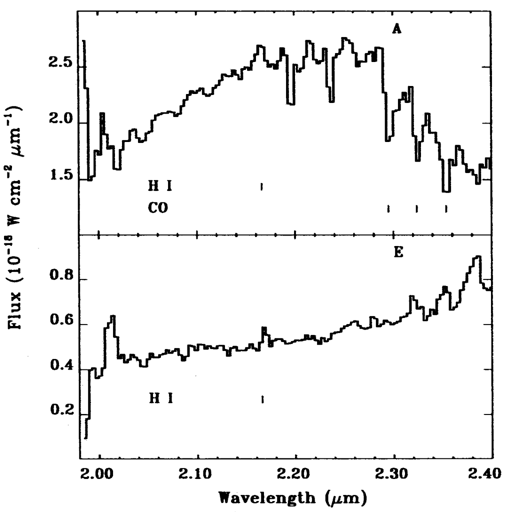

FIG. 5*d*

WR 108, are presented. The similarity is striking. Both show the Brγ and He I (2.112/3 μm) lines, the series of Brackett lines in the *H* band, the He I (1.700 μm) line at $\sim 3\ \sigma$, and *no* He I (2.058 μm line). The difference in the slopes of the spectra is the result of extinction.

Recent work by Conti et al. (1995) shows that Of stars have similar emission lines as WN 7 stars and the G0.12+0.02 cluster stars. The Of stars have the Brγ (2.166 μm) and He I–N III (2.113 μm) in emission, and two of the Of stars in Conti et al., HD 16691 O4 If$^+$ and HD 190429 O4 If$^+$, also have the He II (2.189 μm) in emission. Additional Of stars in Conti et al. have the He II 2.189 μm line in absorption. Their spectra are at a higher resolution than those of the G0.12+0.02 cluster stars, and the absorption features they see would likely go undetected at our resolution. One apparent difference in the Of spectra of Conti et al. and the G0.12+0.02 cluster stars seems to be the amount of line broadening. As seen from our spectra (Fig. 6*a*), the emission lines of the Of?p star HD 148937 are not resolved, whereas the cluster star emission lines are resolved (see § 4.2). Although the Of stars have outflow velocities equal to or exceeding the WN stars (Crowther, Hillier, & Smith 1995), the widths of the detected emission lines in WN and O stars are also sensitive to the effects of the wind densities (e.g., Morris et al. 1993). The lower wind densities in Of stars result in narrower emission lines, and the higher wind densities in WN stars produce broader lines (Morris 1995). Therefore, the broader lines which are seen in the G0.12+0.02 cluster stars seem to recommend the WN classification.

3.3. *The Pistol and AFGL 2004*

The Brγ emission image of the region surrounding the Pistol (Fig. 3) reveals fewer compact sources of strong line emission than seen in the G0.12+0.02 cluster, but it does show extended emission from the Pistol itself. A strong compact emission source is apparent below the Pistol: we denote this as source A. The spectrum of this probable star is very similar to the spectrum of He 3–1191, a B[e] star (see Fig. 8). Line fluxes of both stars are given in Table 3. The only apparent *K*-band line is Brγ. In the *H* band, both source A and He 3–1191 show a strong emission line at ~ 1.69 μm which is most likely the same line identified in η Carinae by Allen, Jones, & Hyland (1985) as the 1.688 μm Fe II (z^4F_9–c^4F_9) line. Additional iron lines in the spectrum of η Carinae have a significantly smaller line flux and therefore are unlikely to be detected in our spectra. Another possible identification of the 1.69 μm line is He II (1.692 μm); however, no other H II lines are apparent in either star.

The two sources directly above the Pistol in Figure 3 correspond (from right to left) to stars 8 and 10 of Glass et al. (1990). The spectra of these stars are presented in Figure 9, and their line fluxes are listed in Table 3. As can be seen,

TABLE 2

G0.12+0.2 Cluster Star Line Fluxes (10^{-21} W cm^{-2})

λ (μm)	Transition	Star: 1[a]	2	3	4	5	6[a]	7	8	9	10	11	12	13
1.611	H (13–4), He I (13–4)	...	...	...	...	...	...	...	...	...	...	1.4 ± 0.6	...	...
1.641	H (12–4), He I (12–4)	...	1.8 ± 0.6	0.6 ± 0.2	...	1.7 ± 0.5	...	1.1 ± 0.2	2.8 ± 0.7	1.8 ± 0.5	2.5 ± 1.0	2.4 ± 0.6	...	...
1.681	H (11–4), He I (11–4)	...	1.5 ± 0.5	0.4 ± 0.2	...	1.7 ± 0.5	...	1.8 ± 0.5	2.7 ± 0.7	2.6 ± 0.6	1.8 ± 0.8	1.9 ± 0.6	...	...
1.700	He I ($4d^3D$–$3p^3P^0$)	...	1.7 ± 0.5	...	...	...	...	...	1.8 ± 0.7	...	...	1.4 ± 0.5	...	...
1.736	H (10–4), He I (10–4)	...	6.2 ± 0.7	1.5 ± 0.3	...	3.0 ± 0.5	...	1.3 ± 0.2	7.3 ± 0.8	5.6 ± 0.6	4.1 ± 1.0	5.2 ± 0.7	...	7.7 ± 1.1
2.112, 2.113	He I ($4s^3S$–$3p^3P^0$), He I ($4s^1S$–$3p^1P^0$)	1.6 ± 0.3	19 ± 2	5.1 ± 0.7	0.7 ± 0.3	4.1 ± 0.6	7 ± 2	1.0 ± 0.2	4.4 ± 0.7	1.8 ± 0.3	1.0 ± 0.2	0.9 ± 0.2	...	2.0 ± 0.4
2.166	H (7–4), He I (7–4)	3.6 ± 0.3	34 ± 2	9.5 ± 0.9	0.9 ± 0.3	8.8 ± 0.6	29 ± 3	2.6 ± 0.2	16 ± 1	7.2 ± 0.4	2.5 ± 0.2	7.0 ± 0.3	0.42 ± 0.09	5.8 ± 0.4
2.189	He II (10–7)	...	5 ± 2	1.2 ± 0.6	...	...	...	...	...	...	...	...	...	...
1.65	Continuum[b]	...	36.2 ± 0.3	11.5 ± 0.3	13.2 ± 0.3	20.0 ± 0.3	...	13.6 ± 0.3	34.2 ± 0.6	27.2 ± 0.4	2.8 ± 0.1	3.1 ± 0.1	3.3 ± 0.1	4.1 ± 0.1
2.20	Continuum[b]	17.6 ± 0.5	80.9 ± 0.4	33.7 ± 0.7	18.7 ± 0.5	39.2 ± 0.6	78.9 ± 0.9	17.1 ± 0.3	45.2 ± 0.6	25.2 ± 0.4	8.5 ± 0.1	13.3 ± 0.2	5.7 ± 0.2	19.6 ± 0.3

[a] No *H* band data available.
[b] Flux in 10^{-19} W cm^{-2} μm^{-1}.

TABLE 3

Pistol Stars and Optically Classified Star Line Fluxes (10^{-20} W cm^{-2})

λ (μm)	Transition	AFGL 8[a]	AFGL 10[a]	Source A	Source B[a]	HD 1489437 (Of?p)	WR 40 (WN 8)	WR 71 (WN 6)	WR 82[a] (WN 8)	WR 108 (WN 9)	He 3–1191 (B[e])
1.570	H (15–4), He I (15–4)	...	...	1.8 ± 0.8	...	13 ± 4	36 ± 7	...	...	3.4 ± 1.0	1.6 ± 0.6
1.572	He II (13–7)	...	...	...	...	...	...	9.2 ± 0.3	...	...	...
1.588	H (14–4), He I (14–4)	...	...	1.7 ± 0.7	...	17 ± 4	36 ± 6	...	...	4.6 ± 1.2	1.7 ± 0.6
1.611	H (13–4), He I (13–4)	...	...	1.4 ± 0.7	...	...	...	...	...	6.1 ± 1.3	...
1.641	H (12–4), He I (12–4)	...	...	4.8 ± 0.9	...	12 ± 4	43 ± 7	...	...	...	3.1 ± 0.7
1.681	H (11–4), He I (11–4)	...	...	7.3 ± 0.9	...	12 ± 5	66 ± 7	...	...	6.1 ± 1.3	3.8 ± 0.6
1.688	Fe II (z^4F_9–c^4F_9)	...	...	8.5 ± 0.8	...	...	...	...	...	...	5.0 ± 0.6
1.692	He II (12–7)	...	...	...	...	...	...	7.4 ± 0.3	...	...	...
1.700	He I ($4d^3D$–$3p^3P^0$)	...	...	...	...	...	178 ± 8	...	...	3.2 ± 1.0	...
1.736	H (10–4), He I (10–4)	...	...	12.4 ± 1.0	...	18 ± 5	112 ± 8	6.3 ± 0.3	...	7.7 ± 1.3	6.2 ± 0.9
2.037	He II (15–8)	...	...	...	...	...	...	0.8 ± 0.1	0.6 ± 0.1	...	...
2.058	He I ($2p^1P^0$–$2s^1S$)	2.1 ± 3	3.5 ± 0.3	...	...	...	16 ± 1	...	0.3 ± 0.1	...	...
2.112, 2.113	He I ($4s^3S$–$3p^3P^0$), He I ($4s^1S$–$3p^1P^0$)	...	0.7 ± 0.3	...	0.7 ± 0.2	15 ± 4, 10 ± 1	24 ± 2	1.2 ± 0.2	2.6 ± 0.2	16.4 ± 1.2, 16.0 ± 1.6	...
2.166	H (7–4), He I (7–4)	1.3 ± 0.3	2.0 ± 0.3	12.3 ± 0.7	1.4 ± 0.2	44 ± 4, 21 ± 1	55 ± 2	1.4 ± 0.2	4.9 ± 0.2	23.6 ± 2.1, 25.0 ± 1.6	7.8 ± 0.6
2.189	He II (10–7)	...	...	...	...	...	5 ± 1	2.6 ± 0.2	2.2 ± 0.2	...	...
2.347	He II (13–8)	...	...	...	...	...	...	1.2 ± 0.2	0.8 ± 0.1	...	...
1.65	Continuum[b]	...	...	3.76 ± 0.08	...	47.8 ± 0.9	39 ± 6	47.8 ± 0.9	...	8.5 ± 0.1	4.37 ± 0.05
2.20	Continuum[b]	0.79 ± 0.02	1.07 ± 0.08	4.8 ± 0.3	0.57 ± 0.02	32.6 ± 0.4, 14.8 ± 0.1	4.9 ± 0.1	0.34 ± 0.01	0.65 ± 0.01	7.5 ± 0.1, 8.6 ± 0.1	7.7 ± 0.2

[a] No *H* band data available.
[b] Flux in 10^{-17} W cm^{-2} μm^{-1}.

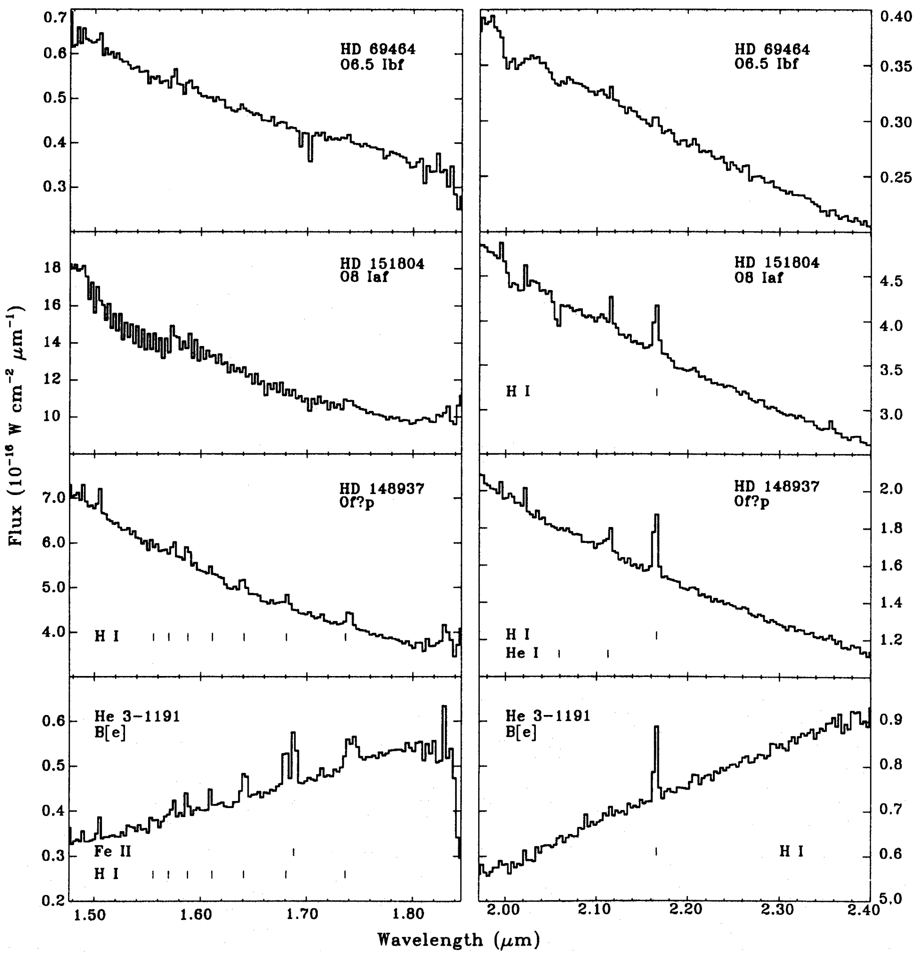

FIG. 6*a*

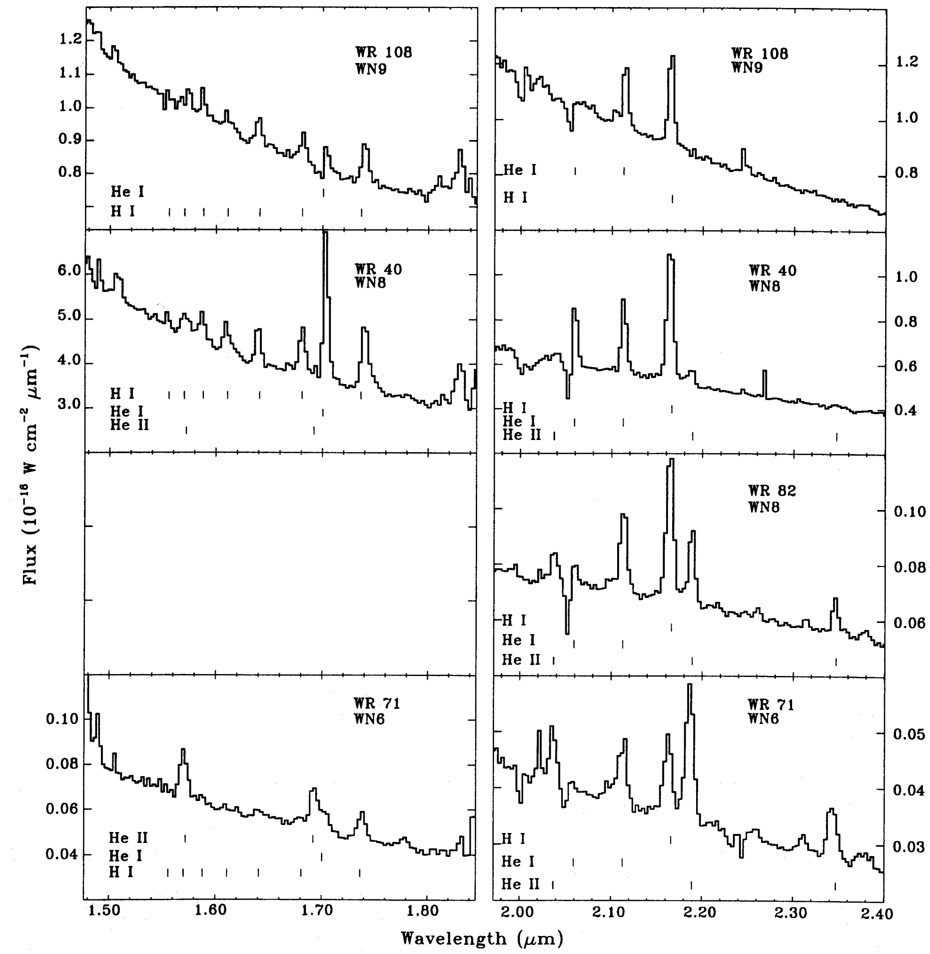

FIG. 6*b*

FIG. 6.—(*a*) *H*- and *K*-band spectra of optically classified stars. (*b*) *H*- and *K*-band spectra of optically classified WN stars.

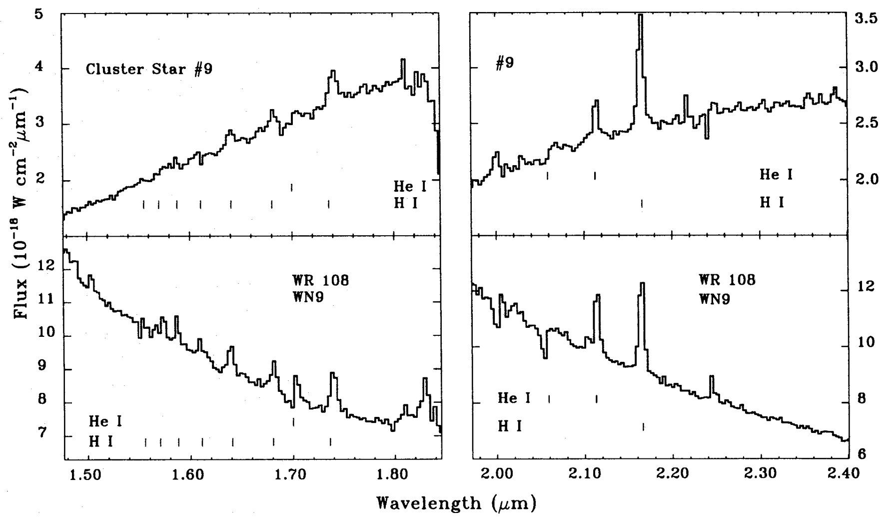

FIG. 7.—*H*- and *K*-band spctra of a typical cluster emission star (No. 9) and WR 108 a type WN 9 star. In the *K* band, the He I (2.112/3 μm) and the Brγ (2.166 μm) lines are clearly seen in emission.

these two stars differ from the G0.12+0.02 cluster stars in the appearance of a strong He I 2.058 μm line and a much weaker He I 2.112/3 μm line. The spectra of these stars are similar to stars in the cluster of He I stars located in the central parsec of the Galaxy (Krabbe et al. 1991). Specifically, the better studied AF star also has He I (2.058)/Brγ (2.166) > 1 (Najarro et al. 1994; Allen et al. 1990; Forrest et al. 1987) and a relatively weak He I 2.112/3 μm line. In addition, in the upper left corner of Figure 3, there is another emission-line star which has not been previously identified: we denote this source as source B. This star (Fig. 9) appears to have a *K*-band emission spectrum similar to the G0.12+0.02 cluster stars. The spectra of the AFGL 2004 emission stars and source B were extracted from the data cube and are therefore at a lower resolution.

4. DISCUSSION

4.1. *Spectral Classification*

From a comparison of *H*- and *K*-band emission lines in the G0.12+0.02 cluster stars with optically classified stars (i.e., Figs. 7 and 8), a spectral identification of WN 8–WN 9 seems plausible; however, based on the recent work of Conti et al. (1995) a classification as Of cannot be discounted. The spectra of the remaining O stars taken during our observations do not show helium emission lines, and most do not show hydrogen emission lines (Cotera 1995). Hanson & Conti (1994) have studied the emission and absorption lines of main-sequence O and B stars; in most of their spectra, the He I and Brγ lines are seen in absorption. Only one of their stars, an O7.5 IIIe star (HD 155806), has both He I 2.058 μm and Brγ in emission; however, the two emission lines are of approximately equal strength, and the He I (2.112/3 μm) line of the G0.12+0.02 cluster stars is not apparent.

The spectra of the G0.12+0.02 cluster stars do not correspond well to the type B0–Ofpe/WN 9 emission-line stars observed in the Large Magellanic Cloud (LMC) by McGregor et al. (1988b). In these LMC stars, whenever the He I (2.112/3 μm) line is detected, the He I (2.058 μm) line is also present, usually with a greater line flux. From comparison with the LMC data, however, the two emission-line stars in the AFGL 2004 cluster (numbers 8 and 10) appear to be Ofpe/WN 9 stars, the classification given to the AF star based on both line ratios and detailed stellar model fits (Allen et al. 1990; Najarro et al. 1994). The spectrum of

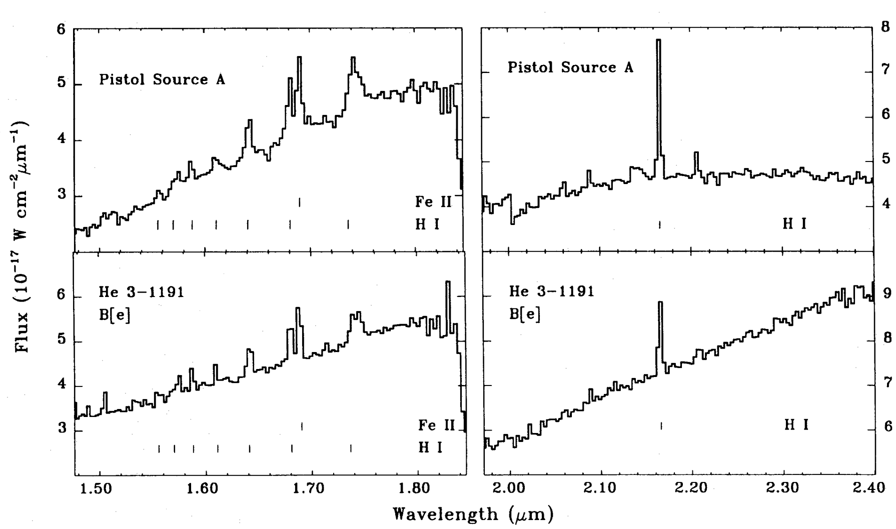

FIG. 8.—Spectra in the *H* and *K* band of the compact source near the Pistol, source A, and He 3–1191, a type B[e] star

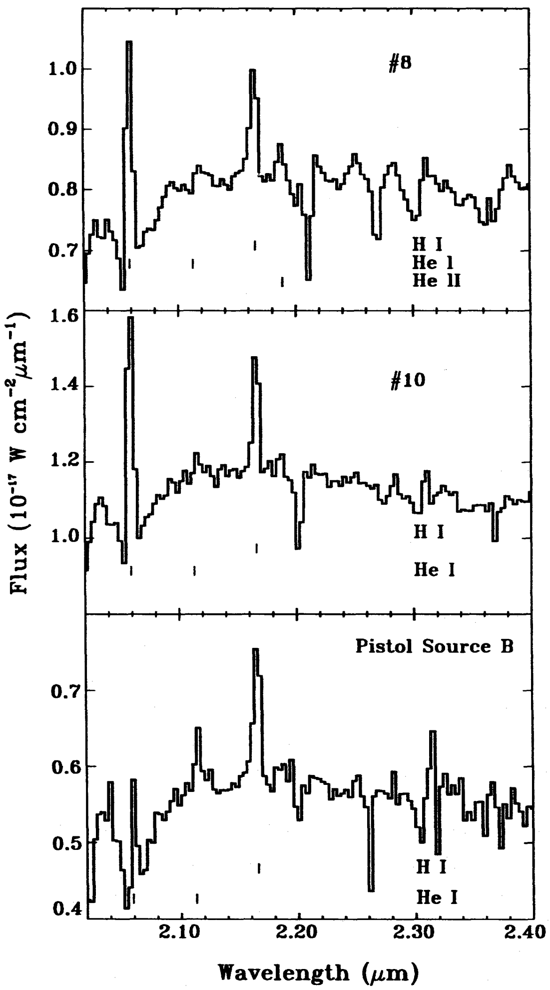

FIG. 9.—The K-band spectra of AFGL 2004 cluster stars 8 and 10 (nomenclature from Glass et al. 1990), and Pistol source B. The He I emission in number 10 has been previously identified by Moneti et al. (1992); the Brγ emission and the spectrum of number 8 are new. The ratio of He I to Brγ is similar to emission stars in Sgr A West.

Pistol source A corresponds best to He 3–1191 (§ 3.3, Fig. 8). He 3–1191 has been classified (Allen 1976a) as a B[e] star, although it has also been suggested that He 3–1191 is a proto–planetary nebula with the circumstellar disk seen edge on (Le Bertre et al. 1989). Comparison of the H- and K-band spectra of Pistol source A and the B[e] stars GG Car and AG Car (Cotera 1995; McGregor, Hyland, & Hillier 1988a) suggests that a preliminary B[e] classification is correct.

Caution should be exercised when using the He I 2.058 μm line, or the lack thereof, in the classification and comparison of stars. The 2.058 μm line is coincident with a telluric absorption line, and atmospheric corrections are not always adequate. This is clearly the case in several of the spectra presented here, especially the spectra of the AFGL 2004 stars 8 and 10. In general, in spectra in which there is a deep telluric absorption feature at 2.01 μm, the 2.058 μm line identification and flux should be treated with skepticism.

4.2. *The* G0.12+0.02 *Emission Stars as WN Stars*

Since hydrogen is present in all of the new stars, it is unlikely that they are early WN stars (WN 2–5) or WC stars, both of which are thought to have little if any remaining hydrogen. On the other hand, the new stars do not seem to be main-sequence O stars, since the O stars do not have strong Brγ emission in conjunction with helium emission (Hanson & Conti 1994; Conti et al. 1993). As noted above, the Of supergiants do sometimes have both the He I 2.112/3 and the He II 2.189 μm emission lines, and the newly discovered G0.12+0.02 cluster stars could be of this type. The spectroscopic evidence that the G0.12+0.02 cluster stars and Pistol source B are late WN stars (WNL) and the AFGL 2004 stars are Ofpe/WN 9 is therefore plausible, but not definitive in light of the possibility of an Of classification and the current incompleteness of NIR spectra of optically classified stars. If the G0.12+0.02 cluster stars are indeed WN stars, then this is an extremely unusual group of stars. There are ~72 known galactic WN stars (Conti 1987), and an additional ~13 such stars in a single cluster is unexpected. An Of classification would make the cluster less startling in this respect and would therefore be a much more comfortable classification.

Examination of Figures 5 and 6 reveals that there is significant line broadening in the Brγ line in both the G0.12+0.02 cluster stars and the WN stars, presumably due to stellar winds. Unbroadened lines in other observed sources imply an instrument FWHM velocity resolution of ~500 km s^{-1}. To find the outflow velocities of the stars, we estimate the full width zero intensity (FWZI) line width in several of the stars and assume $v_\infty \sim v_{\rm FWZI}/2$. This technique may significantly underestimate the actual v_∞, as possible low level wings in the line profile were not taken into account. We find that $v_\infty \sim$ 800–1200 km s^{-1} in the G0.12+0.02 cluster stars and $v_\infty \sim$ 900–1100 km s^{-1} for the optically classified WN stars WR 40, WR 82, and WR 108 (see Table 4) to $\pm$200 km s^{-1}. Hamann, Koesterke, & Wessolowski (1993) found $v_\infty \sim$ 900–1100 km s^{-1} for the same WN stars using a velocity resolution of $\gtrsim$85 km s^{-1} and v_∞ determined from the bases of helium line profiles rather than hydrogen lines.

Assuming that the measured flux at 2.166 μm is due entirely to Brγ, an estimate of the mass-loss rate can be made by using the measured Brγ line flux, F(Brγ), the derived velocities, and the analysis of Simon et al. (1981, 1983) and McGregor et al. (1988a). They assume that the line emission is formed in a spherically symmetric, optically thick, isothermal, ionized flow. Simon et al. (1983) assume a velocity law, $v(r) = v_*(r/r_*)^\eta$, where v_* is the velocity at the stellar surface and, for this analysis, $\eta = 1$. Using the equation for F(Brγ) in McGregor et al. (1988a) and the velocity relation from Simon et al. (1983), we find

$$\dot{M} \propto F({\rm Br}\gamma) D^2 v_\infty^{0.5} \left(\frac{R_*}{R_\infty}\right)^{0.5} \left(\frac{R_*}{R_\odot}\right)^{-0.5} M_\odot\ {\rm yr}^{-1}\ , \quad (2)$$

where R_* is the stellar radius, R_∞ is the radius at which $v = v_\infty$, and D is the distance to the star in kiloparsecs, assumed for the GC to be 8.0 kpc (Reid 1993). F(Brγ), given in Tables 2 and 3, is corrected for extinction assuming $A_K/A_V = 0.11$ (Rieke & Lebofsky 1985) and $A_V = 30$ for the Galactic center. The derived luminosity (see § 4.3) is used to estimate the stellar radius from $L = 4\pi R_*^2 \sigma T^4$ with T = 30,000 K for the cluster stars.

If we assume that (R_*/R_∞) is constant for WNL stars, we can use the above equation, the published mass-loss values for the observed optically classified stars, and our measured values of F(Brγ) to estimate the mass loss for the cluster

TABLE 4

LUMINOSITIES OF OPTICALLY CLASSIFIED STARS

Star	Type	D (kpc)[a]	A_V[a]	$T_{\rm eff}$[a]	log $L/L_\odot$[a]	log $\dot{M}$[a]	v_∞ (km s^{-1})[a]	log $L/L_\odot$[b]	log $\dot{M}$[b]	v_∞ (km s^{-1})[b]
WR 40	WN 8	2.5	1.56	31000	5.3	−4.2	1000	5.3	−4.7	1100
WR 82	WN 8	5.5	4.39	32400	5.4	−4.3	1100	5.3	−4.9	1100
WR 108	WN 9	3.5	4.14	30900	5.8	−4.5	900	5.9	−4.7	900

[a] Hamman et al. 1993.
[b] Derived from our measurements.

stars. To investigate the effectiveness of this analysis technique, we first estimated the mass-loss rate for the optically classified WN stars WR 40, WR 82, and WR 108; the results are presented in Table 4. We found that our technique reproduces the mass loss as determined by Hamann et al. (1993) to within a factor of 2. For the G0.12+0.02 cluster emission-line stars, we determine a mass-loss rate of 9×10^{-6} to 2×10^{-4} $M_\odot$ yr^{-1}. For comparison to another GC star, Najarro et al. (1994) found the mass loss for the AF star, an Ofpe/WN 9 star, to be 6.0×10^{-5} to 9.5×10^{-5} $M_\odot$ yr^{-1}.

4.3. *Stellar Parameters*

The primary difficulty in estimating the stellar parameters of the new stars is the lack of valid detailed models for the infrared spectra of W-R stars. The only model currently available is that of Najarro et al. (1994), which uses the He I (2.058 μm) and Brγ emission line flux, the K-band flux, and the He I (2.058 μm) line profile as constraints. Najarro et al. find that the He I (2.058 μm) line, the 2^1P–2^1S transition, is sensitive to the stellar luminosity and the optical depth of the He I (584 Å) line, the 2^1P–1^1S transition. For a star of fixed $R = 60$ $R_\odot$, when the luminosity becomes sufficient to ionize helium, the optical depth for the He I (584 Å) line is large so almost every recombination to the 2^1P level results in the emission of a He I (2.058 μm) photon. As the luminosity increases further, the He I (2.05 μm) line flux increases, reaching a maximum at the point at which the optical depth of the He I (584 Å) line begins to decrease (the amount of He I is reduced; Najarro et al. 1994). If the luminosity increases beyond this value, the He I (2.058 μm) line flux decreases rapidly. This could explain in part the presence of the He I (2.058 μm) line in the Ofpe/WN 9 stars, which have log $L/L_\odot \sim 5.6$ (McGregor, Hillier, & Hyland 1988b) and the apparent lack of that line in WR 108, a WN 9 star with log $L/L_\odot \sim 5.8$ (Hamann et al. 1993, Fig. 7). However, as seen in Figure 6*b*, the He I (2.058 μm) line is strong in the WN 8–WN 6 stars, but WN 8–WN 6 stars have a luminosity range of $L/L_\odot \sim 5.1$–5.8 (Hamann et al. 1993). Clearly, the investigation of these stars based on their K-band spectra needs further work.

The luminosities of the stars are estimated from the measured continuum flux density, $F(\lambda)$ (W cm^{-2} μm^{-1}) by averaging the results from both 2.2 μm and 1.65 μm, assuming the blackbody relation

$$L = \frac{4\pi^5}{15} F(\lambda) D^2 \lambda^5 e^{\tau_\lambda} \left(\frac{kT_{\rm eff}}{hc}\right)^4 [e^{(hc)/\lambda k T_{\rm eff}} - 1] . \quad (3)$$

Taking $A_V = 30 \pm 5$ for the GC stars, as indicated in Figure 4, and using $A_K/A_V = 0.11$ and $A_H/A_V = 0.16$ (Rieke & Lebofsky 1985), we estimate $\tau_K \sim 3.1$ and $\tau_H \sim 4.8$. To test the accuracy of this technique, we have applied the same technique to the luminosities of WR 108 (WN 9), WR 40 (WN 8), and WR 82 (WN 8) using our values for the continuum flux, and the derived distance, interstellar extinction, and temperatures of Hamann et al. (1993). We compare these luminosities with those in Hamann et al. which were calculated using their derived absolute visual magnitude and an assumed mass-luminosity relationship (Table 4). There is good agreement.

Assuming that the G0.12+0.02 cluster stars and Pistol source B are type WN 9, the AFGL 2004 stars 8 and 10 are type Ofpe/WN 9, and the Pistol source is a type B[e], we take the effective temperatures to be 30,000 K, 25,000 K, and 20,000 K, respectively (Najarro et al. 1994; Hamann et al. 1993; McGregor et al. 1988b; Dachs, Engels, & Kiehling 1988). If the G0.12+0.02 cluster stars are Of stars, $T_{\rm eff}$ would be ∼40,000 K and the corresponding luminosities would be greater. For the assumed spectral type of WN 9, the derived luminosities of the individual G0.12+0.02 cluster stars fall in the range log $L/L_\odot \sim 5.7$–6.8. Although these estimated luminosities are larger than optically studied WNL stars, which have log $L/L_\odot \sim 4.9$–5.9 (Hamann et al. 1993), they are within the range of values for WNL model stars which have an initial mass $\gtrsim 60$ $M_\odot$ (Maeder 1990). The luminosities of the AFGL 2004 stars are log $L/L_\odot \sim 4.3$–4.5, smaller than the derived luminosity of the AF star log $L/L_\odot \sim 5.2$–5.5 (Najarro et al. 1994). The luminosity of Pistol source A is log $L/L_\odot \sim 7.0$, and source B is log $L/L_\odot \sim 6.6$.

The stars must be young, no older than $\sim 10^7$ yr (Chiosi & Maeder 1986), although stellar lifetimes, and the lifetime of the W-R phase, may be increased slightly as a result of metallicity effects (Maeder 1991). The fact that the G0.12+0.02 cluster emission stars appear to be in a common evolutionary state, rather than representing a broad range of W-R evolution, suggests at least three scenarios. (1) The cluster stars were formed at various times with various masses and have coincidently evolved to the same shortlived evolutionary state at the same time. This seems highly improbable. (2) The cluster was formed during a single short burst of star formation, and their initial masses were similar such that they have evolved at a similar rate. The lifetimes of massive WN stars are believed to be $\sim 3 \times 10^5$ yr (Maeder 1991), requiring an extremely short period of star formation. W-R models suggest an initial mass range of 60–120 $M_\odot$ for our derived stellar luminosities (Chiosi & Maeder 1986). This has not been seen elsewhere in the galaxy, although strange and Galactically unique objects seem to be the rule rather than the exception in the GC. The near-simultaneous formation of a tight group of such massive stars seems questionable. (3) The stars were formed at various times but evolved quickly to the WN 8–9 stage, which is a longer lived phase than previously considered, contrary to theoretical models (e.g., Chiosi & Maeder 1986). The current canonical model for Wolf-Rayet stars suggests that the second hypothesis is the most likely, but none of the scenarios are completely satisfactory. If the cluster stars are Of stars, the possibility of scenario (2) being the correct one is enhanced, as the time spent in the Of phase is much greater.

A lower limit for the total mass of the cluster can be derived from dynamical considerations. In order for the stars to withstand the tidal disruption forces from the mass within the Galactic center, the following must hold:

$$\frac{m_{\rm cluster}}{r^3_{\rm cluster}} > \frac{2M_{\rm GC}}{R^3_{\rm GC}} . \quad (4)$$

Assuming $M_{\rm GC} \sim 10^8\ M_\odot$ (Genzel et al. 1994), a projected distance $R_{\rm GC} \sim 25$ pc, and $r_{\rm cluster} \sim 0.6$ pc (15″ at 8.0 pc), the total mass of the cluster must be at least 2400 $M_\odot$. Under the assumption that the initial masses of the observed emission-line stars in the cluster are $\sim 60\ M_\odot$ each, together they would account for $\sim 800\ M_\odot$, which leaves a significant amount of mass required to maintain the cluster against tidal disruption. Additional stars are apparent in broadband images of the cluster (Fig. 1), and from gravitational considerations they are required, suggesting that additional massive stars are likely to be present.

4.4. *Ionization of the Arched Filaments*

4.4.1. *E1 and E2 Filaments*

Assuming that the G0.12+0.02 cluster emission-line stars have $T_{\rm eff} \sim 30{,}000$ K, their total luminosity is log $L/L_\odot \sim 7.4$. This estimate, however, does not take into account the luminosity from stars in the cluster which do not show emission lines, such as G0.12+0.02 cluster star E. Although our images are confusion limited, we can distinguish at least 17 stars within the ∼30″ (1.2 pc) diameter of the G0.12+0.02 cluster, only 13 of which have helium and/or hydrogen emission lines. As main-sequence OB stars do not have significant emission lines in the *H* and *K* bands (e.g., Fig. 6a; Hanson & Conti 1994), the remainder of the cluster stars could be of this type, thereby increasing the total luminosity of the cluster. Using the total luminosity of the G0.12+0.02 cluster emission-line stars and the LTE stellar atmosphere models of Kurucz (1979) assuming a temperature of $T_{\rm eff} = 30{,}000$ K, the cluster stars would produce $N_{\rm Lyc} \sim 2 \times 10^{50}\ {\rm s}^{-1}$ ionizing photons. From numerical integration of the blackbody function, we calculate $N_{\rm Lyc} \sim 5 \times 10^{50}\ {\rm s}^{-1}$ ionizing photons from the cluster emission-line stars at the assumed temperature. Neither the LTE assumption nor the blackbody assumption is a particularly good assumption for massive stars, so the calculated values should be treated cautiously. Based on the Sofue et al. (1986) single-dish radio map, the total radio emission at 43 GHz is 18 Jy for the region including the E1 and E2 filaments, which corresponds to $N_{\rm Lyc} \sim 2 \times 10^{50}\ {\rm s}^{-1}$ required to maintain the ionization of these regions. Thus, under the more conservative value of $N_{\rm Lyc}$ from the cluster emission-line stars, if all the ionizing photons produced by the cluster were absorbed in the E1 and E2 filaments, they would be just sufficient to ionize the entire region. However, geometrical dilution and local extinction have not been taken into account. If the cluster emission stars are Of stars, $T_{\rm eff}$ would be much larger, and the corresponding total ionizing radiation would be greater. The cluster emission stars are therefore likely to be a significant source of ionization for the E1 and E2 filaments, but not the only source.

Assuming that W-R/O in the neighborhood of the G0.12+0.02 cluster is similar to a galactic OB association, ∼0.15 (Maeder 1991; Leitherer 1991), there would be approximately 80 O stars near the cluster which could provide additional ionizating radiation. The unusual nature of the cluster suggests, however, W-R/O will not be typical. The assumed W-R/O requires a normal distribution of stars, although it has been suggested (Morris 1993) that the initial mass function (IMF) of the GC is skewed toward the formation of massive stars owing to the high critical densities required for gravitationally bound clouds in the GC (Güsten & Downes 1980). Erickson et al. (1991) have suggested that ∼50 ZAMS O stars distributed along the E2 filament could produce the required UV ionizing radiation. The existence of any additional O stars will be difficult to verify, as their absorption and emission lines have a much lower signal-to-noise ratio than lines observed to date, and photometric techniques are not able to unambiguously identify these stars.

4.4.2. *The Pistol*

Morphologically and energetically, it is likely that Pistol source A is responsible for the ionization of the Pistol. The position of the source corresponds with a peak in the radio emission and the derived luminosity, log $(L/L_\odot) \sim 7.0$ (using our preliminary classification of the star as B[e] with $T_{\rm eff} \sim 20{,}000$ K), suggests that it dominates the energetics in that area. The extremely large luminosity, in conjunction with a slightly enhanced spatial extent in the Brγ image relative to the emission-line stars in AFGL 2004 (see Fig. 3), suggests that the source may contain more than one star, although broadband images show a spherically symmetric source. From the radio map at 6 cm (Yusef-Zadeh & Morris 1987a), the Pistol has a strength of 0.48 Jy, which converts to $N_{\rm Lyc} \sim 7.5 \times 10^{48}\ {\rm s}^{-1}$. Using a numerical integration of the blackbody function, Pistol Source A could produce $N_{\rm Lyc} \sim 4 \times 10^{50}\ {\rm s}^{-1}$ based on its continuum luminosity. Comparison of the blackbody function and stellar atmosphere models indicates that the blackbody assumption overestimates the ionizing radiation below $T_{\rm eff} \sim 31{,}000$ K by at least an order of magnitude (Panagia 1973). However, the B[e] spectrum is believed to be produced in the envelope of a star which, although usually a main-sequence B star, is not limited to the main-sequence or B-type stars (Underhill & Doazen 1982). Thus, although source A is spectroscopically similar to B[e] stars, the central ionizing source could be much hotter than 20,000 K or be the result of multiple stars. From the ability of source A to provide sufficient ionizing radiation at its minimum temperature, we believe Pistol source A is very likely responsible for the ionization of the Pistol. This is in agreement with the finding of Harris et al. (1994), who suggest that the stars near the Pistol are sufficient to ionize the Pistol and possibly G0.18−0.04, the "Sickle."

5. CONCLUSIONS

The discovery of hot emission-line stars near the Arched Filaments and the Pistol is the first direct evidence that stellar sources could ionize these regions. The G0.12+0.02 cluster of stars, along with the stars near the Pistol, have been shown to be plausible sources of at least partial ionization for their respective radio emission regions. The remaining filaments, E1, W1, and W2, have yet to be investigated for the presence of emission-line stars, but additional emission-line stars have been located near Sgr A East and in between Sgr A and the Arched Filaments (Cotera 1995), and the possibility remains of more emission stars in or near the other filaments. Therefore, the evidence points to at least partial stellar ionization of the thermal emission regions near the Galactic center.

The newly discovered stars are highly unusual objects. Like the cluster of stars within the central parsec of the Galaxy, they are extremely luminous and massive stars. If the G0.12+0.02 cluster of stars are type WN 8–9, and the AFGL 2004 emission stars are Ofpe/WN 9, they are young stars, $\tau_{\rm lifetime} \lesssim 10^7$ yr, supporting a hypothesis of recent star formation in the GC. In addition, if the G0.12+0.02 cluster stars are in fact WN stars, they represent ~14% of all known galactic WN stars (Hamann et al. 1993). Improving our understanding of their formation in the unique conditions of the Galactic center should lead to a better grasp of the energetics in that region of the galaxy and possibly the nature of W-R stars.

A. S. C. acknowledges support from the NASA Graduate Student Research Program Minority Focus Component; S. W. J. C. and J. P. S. acknowledge NASA-Ames Research Center Interchange Grants NCC 2-647 and NCC 2-548, respectively. The authors would like to thank the staff at the Anglo-Australian Observatory for extensive help in obtaining, reducing, and presenting the data for this paper. We also thank the referee for his helpful comments.

REFERENCES

Allen, C. W. 1976a, Astrophysical Quantities (London: Athlone)
Allen, D. A. 1976b, MNRAS, 174, 29P
———. 1994, in The Nuclei of Normal Galaxies, NATO ASI Ser. C, Vol. 445, ed. R. Genzel & A. I. Harris (Dordrecht: Kluwer), 293
Allen, D. A., & Craig, T. A. 1983, MNRAS, 203, 777
Allen, D. A., Hyland, A. R., & Hillier, D. J. 1990, MNRAS, 244, 706
Allen, D. A., Jones, T. J., & Hyland, A. R. 1985, ApJ, 291, 280
Burton, M. G., & Allen, D. A. 1992, Proc. Astron. Soc. Australia, 10, 55
Catchpole, R. M., Whitelock, P. A., & Glass, I. 1990, MNRAS, 247, 479
Chiosi, C., & Maeder, A. 1986, ARA&A, 24, 329
Conti, P. S. 1987, ARA&A, 25, 113
Conti, P. S., Block, D. L., Geballe, T. R., & Hanson, M. M. 1993, ApJ, 406, L21
Conti, P. S., Hanson, M. M., Morris, P. W., Willis, A. J., & Fossey, S. 1995, ApJ, 445, L35
Cotera, A. S. 1995, Ph.D. thesis, Stanford Univ.
Cotera, A. S., Erickson, E. F., Simpson, J. P., Colgan, S. W. J., & Rieke, M. 1992, BAAS, 24, 765
Crowther, P. A. 1995, private communication
Crowther, P. A., Hillier, D. J., & Smith, L. J. 1995, A&A, 293, 172
Dachs, J., Engels, D., & Kiehling, R. 1988, A&A, 194, 167
Erickson, E. F., Colgan, S. W. J., Simpson, J. P., Rubin, R. H., Morris, M., & Haas, M. R. 1991, ApJ, 370, L69
Forrest, W., Shure, M. A., Pipher, J. L., & Woodward, C. E. 1987, in The Galactic Center, ed. D. C. Backer (New York: AIP), 153
Genzel, R., Hollenbach, D., & Townes, C. H. 1994, Rep. Prog. Phys., 57, 417
Glass, I., Moneti, A., & Moorwood, A. 1990, MNRAS, 242, 55p
Güsten, R., & Downes, D. 1980, A&A, 87, 6
Hamann, W. R., Koesterke, L., & Wessolowski, U. 1993, A&A, 274, 397
Hanson, M. M., & Conti, P. S. 1994, ApJ, 423, L139
Harris, A., et al. 1994, in The Nuclei of Normal Galaxies, NATO ASI Ser. C, Vol. 445, ed. R. Genzel & A. I. Harris (Dordrecht: Kluwer), 223
Hillier, D. J. 1985, AJ, 90, 1514
Krabbe, A., Genzel, R., Drapatz, S., & Rotaciuc, V. 1991, ApJ, 382, L19
Kurucz, R. L. 1979, ApJS, 40, 1
Le Bertre, T., Epchtein, N., Gouiffess, C., Heydari-Malayeri, M., & Perrier, C. 1989, A&A, 225, 417
Leitherer, C. 1991, in IAU Symp. 143, Wolf-Rayet Stars and Interrelations with other Massive Stars in Galaxies, ed. K. A. Van Der Hucht & B. Hidayat (Dordrecht: Kluwer), 465
Maeder, A. 1990, in STSCI Symposium Series 5, Massive Stars in Starbursts, ed. C. Leitherer, N. R. Walborn, T. M. Heckman, & C. A. Norman (Cambridge: Cambridge Univ. Press), 97
Maeder, A. 1991, in IAU Symp. 143, Wolf-Rayet Stars and Interrelations with other Massive Stars in Galaxies, ed. K. A. Van Der Hucht & B. Hidayat (Dordrecht: Kluwer), 445
McGregor, P. J., Hillier, D. J., & Hyland, A. R. 1988b, ApJ, 334, 639
McGregor, P. J., Hyland, A. R., & Hillier, D. J. 1988a, ApJ, 324, 1071
Moneti, A., Glass, I., & Moorwood, A. 1992, MNRAS, 258, 705
———. 1994, MNRAS, 268, 194
Morris, M. 1989, in IAU Symp. 136, The Center of the Galaxy, ed. M. Morris (Dordrecht: Kluwer), 171
———. 1993, ApJ, 408, 496
Morris, M., Davidson, J. A., Werner, M., Dotson, J., Figer, D. F., Hildebrand, R., Novak, G., & Platt, S. 1992, ApJ, 399, L63
Morris, M., & Yusef-Zadeh, F. 1989, ApJ, 343, 703
———. 1985, AJ, 90, 2511
Morris, P. 1995, private communication
Morris, P., Conti, P. S., Lamers, H. J. G. L. M., & Koenigsberger, G. 1993, ApJ, 414, L25
Nagata, T., et al. 1990, ApJ, 351, 83
Najarro, F., Hillier, D. J., Kudriski, R. P., Krabbe, A., Lutz, D., Genzel, R., Drapatz, S., & Geballe, T. R. 1994, A&A, 285, 573
Okuda, H., et al. 1990, ApJ, 351, 89
Panagia, N. 1973, AJ, 78, 929
Rieke, G. H., & Lebofsky, M. J. 1985, ApJ, 288, 618
Reid, M. J. 1993, ARA&A, 31, 345
Serabyn, E., & Güsten, R. 1987, A&A, 184, 133
———. 1991, A&A, 242, 376
Simon, M., Felli, M., Cassar, L., Fischer, J., & Massi, M. 1983, ApJ, 266, 623
Simon, M., Righini-Cohen, G., Fisher, J., & Cassar, L. 1981, ApJ, 251, 552
Sofue, Y., Inoue, M., Handa, T., Tsuboi, M., Hirabayashi, H., Morimoto, M., & Akabane, K. 1986, PASJ, 38, 475
Underhill, A., & Doazan, V. 1982, B Stars With and Without Emission Lines (Washington: NASA SP-465)
van der Hucht, K. A., Conti, P. S., Lundström, I., & Stenholm, B. 1981, Space Sci. Rev., 28, 227
Wainscoat, R. J., & Cowie, L. L. 1992, AJ, 103, 332
Yusef-Zadeh, F., & Morris, M. 1987a, AJ, 94, 1178
———. 1987b, ApJ, 322, 721
Yusef-Zadeh, F., Morris, M., & Chance, D. 1984, Nature, 310, 557